[Frontiers in Bioscience, Landmark, 21, 343-363, January 1, 2016]

Differential proteome analysis along jejunal crypt-villus axis in piglets

Xia Xiong[1], Huansheng Yang[1,7], Xihai Hu[6], Xiaocheng Wang[1], Biao Li[1], Lina Long[1], Tiejun Li[1], Junjun Wang[3], Yongqing Hou[4], Guoyao Wu[3-5], Yulong Yin[1,2,4]

[1]Chinese Academy of Science, Institute of Subtropical Agriculture, Research Center of Healthy Breeding Livestock and Poultry, Human Engineering and Research Center of Animal and Poultry Science, Key Lab Agroecology Processing Subtropical Region, Scientific Observational and Experimental Station of Animal Nutrition and Feed Science in South-Central, Ministry of Agriculture, Changsha City, Hunan, 410125, People's Republic of China, [2]School of Life Sciences, Hunan Normal University, Changsha 410008, [3]State Key Laboratory of Animal Nutrition, China Agricultural University, Beijing, People's Republic of China 100193, [4]Hubei Key Laboratory of Animal Nutrition and Feed Science, Wuhan Polytechnic University, Wuhan 430023, People's Republic of China, [5]Department of Animal Science, Texas A and M University, College Station, TX 77843, USA, [6]Hunan agricultural university, Changsha, Hunan P.R. China, [7]Fujian Aonong Biotechnology Corporation, Xiamen, Fujian, 361007, P. R. China

TABLE OF CONTENTS

1. ABSTRACT

The brush-border membrane (BBM) of enterocytes is responsible for the digestion and absorption of nutrients and ions in the small intestine. To identify the BBM proteins involved in epithelial cell maturation along the crypt-villus axis, enterocytes were sequentially isolated from the villus tip to the crypt of the jejunum from 21-day-old suckling piglets. After preparation of BBM vesicles, we detected 194 proteins in the jejunal epithelial cells by isobaric tags using relative and absolute quantification (iTRAQ) techniques. Of these, 56 BBM proteins were differentially expressed along the crypt-villus axis. During differentiation, the expression of proteins related to digestion and absorption of nutrients was primarily downregulated at the upper, middle villus, or crypt compared to the villus tip, while expression of proteins related to structural and enzyme regulator proteins was largely upregulated. We verified the differences in Na^+/K^+ -transporting ATPase, galectin-3, and an intestinal-type fatty acid binding protein by western blot or immunochemical analysis. Identification of BBM-associated proteins helps enhance our understanding of digestion and absorption in piglets and other mammals, including humans.

2. INTRODUCTION

The postnatal development of the gastrointestinal system is a very dynamic process, and gastrointestinal

organs grow faster than many other organs of the body during the suckling period (1,2). The main function of the small intestine involves the absorption of nutrients arising from intestinal digestion. The small intestinal epithelium continuously and rapidly regenerates itself (3). This dynamic system involves proliferation of stem cells located at the bottom of the crypt, cell population expansion in the mid-villus, terminal differentiation in the upper villus, and extrusion of the senescent cells at the tip of the villus (4). Thus, cell localization along the crypt-villus axis is highly hierarchized and reflects a differential potential for key phenomena, such as proliferation, migration, and tissue-specific gene expression (5,6).

The brush-border membrane (BBM) of enterocytes that line the villus is exposed to the luminal gastrointestinal content, which is equipped with diverse enzymes and nutrient transporters, as well as a complex network of cytoskeletal proteins that anchor the membrane and contribute to its characteristic "ruffled" appearance (7). Characterization of the proteins in BBM along the crypt-villus axis may help improve our understanding of the functions of enterocytes and provide insight into the regulators of intestinal cell maturation. The aim of the current study was to investigate the differential expression of BBM-associated proteins along the crypt-villus axis in jejunum of 21-day-old suckling piglets by isobaric tag relative and absolute quantification (iTRAQ) coupled with liquid chromatography-tandem mass spectrometry (LC-MS/MS) proteomics.

3. MATERIALS AND METHODS

3.1. Reagents

DL-β-Hydroxybutyrate sodium salt was purchased from J&K Chemical (Ltd., USA). Trypsin was procured from Promega (Madison, WI, USA). iTRAQ-reagent was purchased from Applied Biosystems (Foster City, CA, USA). Bovine serum alumin (BSA, fraction V), phenylmethylsulfonyl fluoride (PMSF), dithiothreitol (DTT), and other chemical were obtained from Sigma-Aldrich (St. Louis, MO, USA).

3.2. Sequential isolation of epithelial cells along the crypt-villus axis

Eight 21-day-old suckling piglets (Duroc × Landrace × Yorkshire) were sacrificed by CO_2 asphyxiation (8), and jejunal segments were collected for isolation of epithelial cells and immunohistochemical analyses (9). The sequential isolation of pig small intestinal epithelial cells along the crypt-villus axis was based on the method of Fan *et al.* (6). Briefly, the divided mid-jejunum segments were rinsed thoroughly with ice-cold physiological saline solution and incubated at 37 °C for 30 min with oxygenated PBS. The fluid contents of the intestinal segments were drained and discarded. The jejunum segments were then filled with 15–30 mL isolation buffer (5 mM Na_2EDTA, 10 mM HEPES pH 7.4., 0.5. mM DTT, 0.2.5% BSA, 2.5. mM D-glucose, 2.5. mM L-glutamine, 0.5. mM dl-β-hydroxybutyrate sodium salt, oxygenated with an O_2/CO_2 mixture (19:1, v/v)) and incubated for 20 or 30 min in a shaking water bath incubator at 37 °C. After incubation, the contents of the segment, which included buffer and isolated cells, were transferred to a 250-mL conical centrifuge bottle. This procedure was repeated six times to yield six "cell fractions" (F1 to F6). Each of the first two cell fractions (F1 to F2) was collected sequentially after a separate 20-min period of incubation, the second two cell fractions (F3 to F4) was collected sequentially after a separate 25-min period of incubation, and the last two fractions (F5 to F6) was collected sequentially after a separate 30-min period of incubation. The cell fractions were washed twice as follows: each cell fraction was centrifuged at 400 × g for 4 min at 4 °C, the supernatant was discarded, and the cell pellet was dispersed in 15–30 mL of oxygenated cell resuspension buffer (10 mM HEPES, 1.5. mM $CaCl_2$, 2.0. mM $MgCl_2$, pH 7.4.). The cells were immediately frozen at -80 °C for enzyme marker assays and BBM preparation.

The experimental design and procedures used in this study were carried out in accordance with the Chinese Guidelines for Animal Welfare and Experimental Protocols, and approved by the Animal Care and Use Committee of the Institute of Subtropical Agriculture at the Chinese Academy of Sciences (10).

3.3. Preparation of BBM vesicles

Brush-border membrane vesicles were prepared by Mg^{2+} precipitation and differential precipitation, as described previously (7,11). The cell fractions collected from eight piglets with a normal birth weight were resuspended in ice-cold homogenate buffer (100 mM mannitol, 2 mM Tris-HEPES, pH 7.4., 0.1. mM phenylmethylsulfonyl fluoride (PMSF)) and homogenized with a Tissue Tearor (T8 Ultra-Turrax, IKA®-Werke GmbH & Co. KG, Germany). The resulting homogenate was centrifuged at 2,000 × g for 15 min. The supernatant fluid was removed and a solution of 200 mM $MgCl_2$ was added to the remaining supernatant to a final concentration of 10 mM, followed by gentle mixing for 15 min. The suspension was centrifuged again at 2,400 × g for 15 min. The supernatant fluid was obtained and centrifuged at 30,000 × g for 30 min. The resultant pellet was resuspended in buffer (100 mM mannitol, 2 mM Tris-HEPES pH 7.4., 1 mM MgSO4, and 0.1. mM PMSF), homogenized for 1 min, and centrifuged at 2,400 × g for 15 min. The supernatant fluid was then centrifuged at 39,000 × g for 30 min, and the resulting pellet was stored at -80 °C until further use (12).

3.4. Sample preparation and isobaric labeling

The BBM was incubated in lysis buffer (6 M urea, 5 mM EDTA, 0.1.% SDS, 0.1. M triethylammonium bicarbonate pH 8.5.) at 37 °C for 30 min and ultrasonicated

© 1996-2016

(Sonics & Material, Newtown, CT, USA) for 10 min. Trypsin digestion and iTRAQ labeling were performed according to the manufacturer's protocol (Applied Biosystems, Foster City, CA, USA). Briefly, 100 μg total protein of cell fraction was reduced and alkylated, digested overnight at 37 °C with trypsin (Promega, Madison, WI, USA), and labeled with iTRAQ-reagents (Applied Biosystems, Foster City, CA, USA) as follows: F1 (villus tip), iTRAQ reagent 117; F2 (upper villus), iTRAQ reagent 118; F4 (middle villus), iTRAQ reagent 119; F6 (crypt region), iTRAQ reagent 121.

3.5. Peptide fractionation and LC-MS/MS acquisition

The isotopically labeled samples were pooled and fractionated by strong cation exchange chromatography on an LC-20AD HPLC system (Shimadzu Scientific Instruments, Kyoto, Japan), using a polysulfoethyl A column (2.1. × 100 mm, 5 μm, 300 Å; The Nest Group Inc., Southborough, MA, USA), as previously described (13). The eluted fractions were desalted using a Sep-Pak C18 Cartridge (Waters, Milford, MA, USA) and diluted with the loading buffer (10 mM KH_2PO_4 in 25% acetonitrile, pH 2.8.). Buffer A was identical, in composition, to the loading buffer, and buffer B was buffer A with 350 mM KCl. Separation of proteins was performed using a linear binary gradient of 0–80% buffer B in buffer A at a flow rate of 200 μL/min for 60 min. The absorbance at 214 nm and 280 nm was monitored, and a total of 30 fractions were collected along the gradient.

Each elution fraction from the polysulfoethyl A column was dried down, dissolved in buffer C (5% acetonitrile, 0.1.% formic acid), and analyzed on QStar XL (Applied Biosystems), as previously described (13). Briefly, peptides were separated on a reversed-phase (RP) column (ZORBAX 300SB-C18 column, 5 μm, 300 Å, 0.1. × 15 mm; Waters) using an LC-20AD HPLC system (Shimadzu Scientific Instruments). The HPLC gradient was 5–35% buffer D (95% acetonitrile, 0.1.% formic acid) in buffer C at a flow rate of 0.2. μL/min for 65 min. Survey scans were acquired from m/z 400–1800 with up to four precursors selected for MS/MS from m/z 100–2000 using a dynamic exclusion of 30s. The iTRAQ labeled peptides fragmented under collision-induced dissociation conditions to give reporter ions at m/z 117.1., 118.1., 119.1., and 121.1. The ratios of the peak areas of the iTRAQ reporter ions reflect the relative abundances of the peptides and, consequently, the proteins in the samples. Larger, sequence-information-rich fragment ions were also produced under these MS/MS conditions, providing the identity of the protein from which the peptide originated.

3.6. Data analysis and quantification

Database searches to identify the peptides were performed with ProteinPilot™ 3.0. software (Software rev. 114732; Applied Biosystems), using the Paragon and ProGroup algorithms against the NCBI non-redundant database, which contained information on mammalian proteins (31786 sequences). The precursor tolerance was set to 0.2. Da, and the iTRAQ fragment tolerance was set to 0.2. Da. The search parameters were: i) enzyme cleavage by trypsin with one missed cleavage allowed and ii) the fixed modifications of MMTS were set as Cys. An automatic decoy database search strategy was employed to estimate the false discovery rate (FDR). The FDR for the protein identification was calculated by searching against a concatenated reversed database. In the final search results, the FDR was less than 1.5.%. The protein confidence threshold cutoff was 1.3. (Unused ProtScore) from at least two peptides with 95% confidence. For protein identification, the filters were set as follows: significance threshold $P \leq 0.0.5$ (with 95% confidence) and ion score or expected cutoff ≤0.0.5 (with 95% confidence).

3.7. Enzyme activity and western blot analysis

The activities of alkaline phosphatase were determined using an enzyme assay kit, according to the manufacturer's protocol (Nanjing Jiancheng Bioengineering Institute, Nanjing, China). Western blot analysis was performed as described by Xiong *et al.* (14). Ice-cold RIPA lysis buffer (Biyuntian Biotech Co., Ltd., Shanghai, China) containing 0.1. mM PMSF was used to extract total protein from the intestinal epithelial cells. The samples were then centrifuged, and the protein concentration in the resulting supernatant fluid was determined before western blot detection of target proteins. The following primary antibodies were used: anti-PCNA, anti-β-actin, and anti-Na^+/K^+ ATPase (Santa Cruz Biotechnology, Santa Cruz, CA, USA); anti-pan-cadherin (Abcam, Cambridge, UK).

3.8. Immunohistochemistry localization

Jejunal segments from 21-day-old suckling piglets were fixed overnight in 10% neutral buffered formalin and embedded in paraffin. After dewaxing and hydration, 5-μm sections were pretreated with 3% H_2O_2 for 10 min at room temperature, and antigen retrieval was achieved by boiling in 1% citrate at pH 6.0. for 30 min. The sections were blocked with 5% BSA in PBS and incubated with primary antibodies: anti-galectin-3 (1:50 dilution, goat polyclonal, sc-19283, Santa Cruz Biotechnology) and anti-FABP (1:50 dilution, goat polyclonal, sc-16063, Santa Cruz Biotechnology) overnight at 4 °C. After washing with 0.1. M PBST (pH 7.4.) (5 min, 3 washes), antibodies were detected using the Polink-2 Plus Polymer HRP detection system for a goat primary antibody (PV-9003, ZSGB-Bio, Beijing, China) according to the manufacturer's instructions. The reaction was visualized with a 3-3'-diaminobenzidine tetrahydrochloride (DAB) kit (ZLI-9017, ZSGB-Bio). Then, the sections were counterstained with Harris hematoxylin and washed sequentially with 1% hydrochloric acid (prepared with 75% ethanol) and water. After dehydration

© 1996-2016

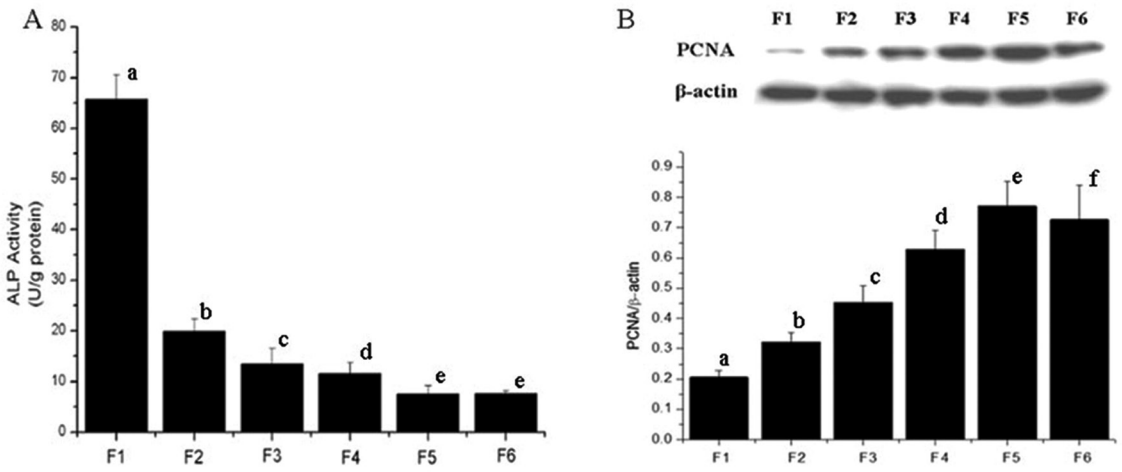

Figure 1. Validation of cell fractions isolated from pig small intestinal crypt-villus axis. (A) ALP activity and (B) PCNA expression along the crypt-villus axis. Values are represented as means ± SEM, n = 8. Values not sharing common superscripted letters are significantly different at P < 0.0.5.

in graded alcohols and clearing with dimethylbenzene, the slides were mounted with neutral gum and examined using the Image-Pro Plus analytical imaging system (Media Cybernetics, Bethesda, MD, USA).

3.9. Statistical analysis

The data on PCNA expression and enzyme activities were analyzed using the t-test in SAS (Version 9.2.; SAS Inst. Inc., Cary, NC, USA). Values are presented as means ± SEM, and probability values < 0.0.5 were taken to indicate statistical significance.

4. RESULTS

4.1. Validation of fractionation procedure

We isolated six cell fractions of small-intestinal epithelial cells from young pigs and validated the efficiency of fractionation by measuring alkaline phosphatase and PCNA, indicators of intestinal cell differentiation and DNA synthesis (Figure 1). The highest activity of alkaline phosphatase was observed in fraction 1 (villus tip), whereas PCNA expression was maximal in fraction 6 (crypt region). These findings demonstrate an efficient fractionation of differentiated villus cells and proliferating crypt cells from the piglet small intestine.

4.2. General profiles of brush-border membrane protein expressions along the crypt-villus axis

A total of 788 proteins were identified in the BBM preparations. Functional annotations of the proteins were performed using the Blast2GO® program against the non-redundant database for mammalian proteins. Of the identified proteins, 194 proteins were localized in BBM (Table 3). The BBM proteins in the jejunum of 21-day-old suckling piglets were classified into 11 groups based on GO function (Figure 2), including enzymes (group 1); structural proteins (group 2); transporters (group 3); binding (group 4); electron carrier activity (group 5); auxiliary transport proteins (group 6); antioxidant reaction (group 7); regulator of metabolic pathways (group 8); transcriptional factors (group 9); chemoattractant response (group 10); and molecular transducers (group 11). The category representing the greatest fraction of BBM proteins was group 4 (46.5.%), comprising proteins involved in binding. Enzymes (group 1; 25.4.%), transporters (group 3; 8%), and regulators of metabolic pathways (group 8; 6%) comprised the next largest fractions. The enzymes and transporter protein were primarily down-regulated along the crypt-villus axis, while structural molecules and regulators of metabolic pathways were mainly upregulated.

4.3. Differentially expressed BBM proteins in the jejunum along the crypt-villus axis

Of the 194 identified BBM proteins, 55 (25.6.%) unique proteins were found to be differentially expressed (P-value < 0.0.5, >1.2.–fold < 0.8., n = 8) along the crypt-villus axis. A total of 30 proteins were down-regulated in the other three fractions of the BBM compared to the villus tip, including those with roles in nutrient digestion (7) as well as in nutrient uptake and ion transport (15) (Table 1). Notably, the expression of chloride intracellular channel protein 5 isoform X2, keratin, type I cytoskeletal 9, PREDICTED: intestinal-type alkaline phosphatase-like isoform 2, and SLC25A5 protein were continuously down-regulated along the crypt-villus axis.

There were 26 BBM proteins in the other three fractions that exhibited higher abundances compared to the villus tip, which largely consisted of signaling proteins and receptors (Table 2). Along the crypt-villus axis, the abundancec of brain-specific angiogenesis

© 1996-2016

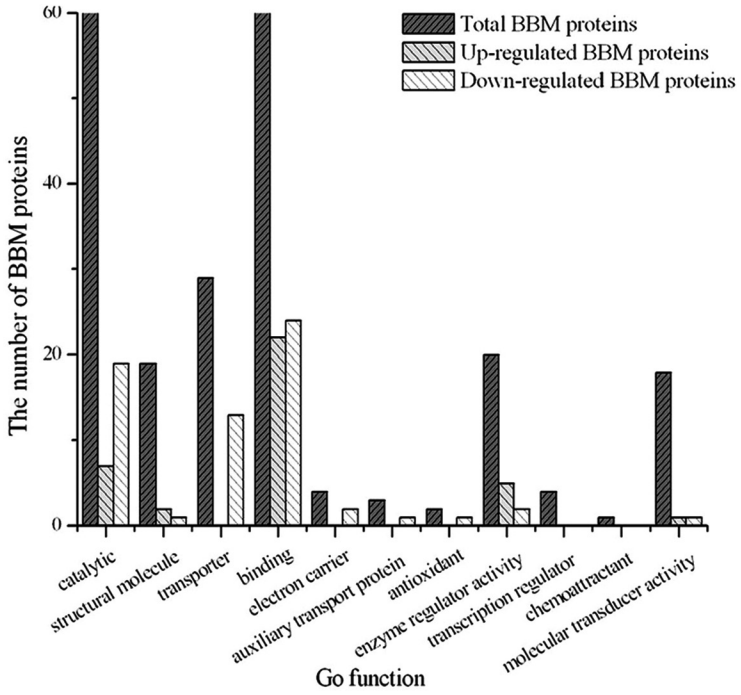

Figure 2. Classification of Go functions of the upregulated and downregulated brush-border membrane proteins in the three jejunal fractions of 21-day-old suckling piglets compared to the villus tip, from iTRAQ (isobaric tags for relative and absolute quantification) data.

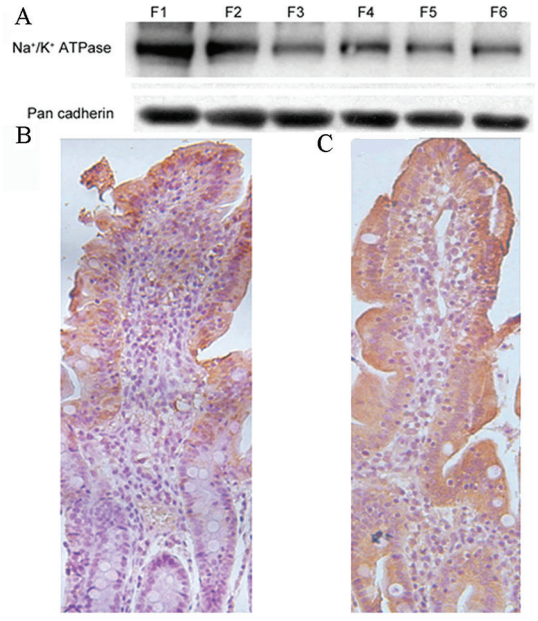

Figure 3. Validation of changes in expression of Na^+/K^+ ATPase, I-FABP, and galectin-3 by western blot or immunohistochemistry. (A) Na^+/K^+ ATPase; (B) I-FABP, and (C) galectin-3. Pan-cadherin served as a loading control.

inhibitor 1-associated protein 2-like protein 1-like and ras GTPase-activating protein-binding protein 1 were continuously upregulated.

4.4. Validation of proteomic changes

Compared to the villus tip, the expression of Na^+/K^+ -transporting ATPase in the upper and middle villus was downregulated in western blot analysis (Figure 3a). The staining patterns of anti-FABP showed higher expression in villus cells compared to the crypt region, which is consistent with the expression changes observed in the proteomic analysis (Figure 3b). In addition, analysis of the immunostaining patterns of galectin, revealed a higher level of its expression in the upper villus than in the villus tip (Figure 3c).

5. DISCUSSION

The growth and ontogenetic development of the pig small intestine is a topologically and temporally organized process, which guides the formation of specialized intestinal epithelium that is defined by a set of genes expressed in different epithelial cells. The identification of proteins unique to the jejunal crypt-villus axis, including digestive enzymes and nutrient transporters, may help elucidate the underlying biological mechanisms responsible for mammalian intestinal differentiation and development. Previous investigations of the expression of genes or proteins in the differentiation process were generally carried out with mice or Caco-2 cell lines (human epithelial cells from colorectal adenocarcinoma) (5,16-19), and few studies focused on the BBM proteome of enterocytes during maturation. The pig is a useful animal model for the study

© 1996-2016

Table 1. Reduced abundances of digestive and transport proteins in the crypt compartment of jejunum at 21-day-old suckling piglets

Protein Name	Biological Process	Fold change (F2)	P-val	Fold change (F4)	P-val	Fold change (F6)
Aminopeptidase N	proteolysis	0.9.91	0.8.14	0.5.11	<0.0.001	
Angiotensin-converting enzyme 2	proteolysis	0.9.46	0.6.27	0.4.13	0.0.001	
Apolipoprotein a-iv	Cholesterol homeostasis	0.8.31	0.0.54	0.8.71	0.2.42	
chloride intracellular channel protein 5 isoform x2	chloride transport	**0.7.24**	0.0.49	**0.3.98**	0.0.09	
Dipeptidase 1 precursor	proteolysis	1.1.58	0.4.82	0.6.48	0.1.09	
Dipeptidyl peptidase 4	proteolysis	0.6.91	0.0.81	**0.5.15**	<0.0.001	
Fatty acid-binding protein, intestinal	fatty acid metabolic	1.4.19	0.1.83	0.5.24	0.3.77	
glycerol-3-phosphate dehydrogenase 1-like protein	triglyceride biosynthetic process	1.0.09	0.9.13	**0.4.92**	0.0.48	
Glutamyl aminopeptidase	proteolysis	0.8.62	0.5.57	**0.4.52**	0.0.001	
keratin, type I cytoskeletal 9	intermediate filament organization	**0.7.94**	0.0.13	**0.0.63**	<0.0.001	
low affinity sodium-glucose cotransporter	carbohydrate transport	1.1.91	0.6.40	0.6.36	0.2.49	
Sodium glucose cotransporter 1	carbohydrate transport	0.9.54	0.9.94	**0.3.83**	0.0.008	
Sodium potassium-transporting atpase subunit alpha-1	ion transport	1.0.0	0.2.92	**0.6.48**	0.0.02	
PREDICTED: canalicular multispecific organic anion transporter 1	ATP catabolic process	0.9.20	0.3.54	**0.6.66**	0.0.06	
PREDICTED: acid sphingomyelinase-like phosphodiesterase 3b	unknown	0.7.94	0.3.07	**0.3.25**	0.0.001	
PREDICTED: 4F2 cell-surface antigen heavy chain	carbohydrate metabolic	1.1.91	0.6.35	0.7.51	0.7.23	
PREDICTED: cadherin-17	oligopeptide transport	1.2.13	0.9.14	**0.5.80**	0.0.35	
REDICTED: intestinal-type alkaline phosphatase-like isoform 2	metal ion binding	**0.6.19**	0.0.10	**0.6.08**	0.0.05	
PREDICTED: meprin A subunit beta	proteolysis	1.3.18	0.0.84	**0.5.64**	0.0.43	
PREDICTED: multidrug resistance protein 1 isoform 2	ATP catabolic process	0.7.65	0.0.78	**0.3.87**	<0.0.001	
PREDICTED: n-acetylated-alpha-linked acidic dipeptidase-like protein	proteolysis	1.0.47	0.9.17	**0.4.24**	0.0.004	
PREDICTED: sodium-coupled monocarboxylate transporter 2	sodium ion transport	1.1.91	0.4.66	0.5.15	0.0.55	
PREDICTED: sucrase-isomaltase, intestinal isoform 1	carbohydrate metabolic	0.9.90	0.3.47	0.4.32	0.0.59	
PREDICTED: solute carrier family 22 member 13	organic cation transport	0.8.16	0.3.46	0.6.13	0.1.82	
PREDICTED: pyruvate kinase isozymes M1/M2 isoform 1	programmed cell death	0.8.95	0.7.73	**0.4.92**	0.0.005	
protein disulfide-isomerase A3	protein folding	**0.3.53**	0.0.08	1.1.27	0.8.22	1.2.47
protein disulfide-isomerase a6	protein folding	**0.4.74**	0.0.34	0.9.72	0.7.42	1.6.59
protein S100-G	calcium ion binding	0.8.01	0.6.78	0.4.83	0.3.06	
Solute carrier family facilitated glucose transporter member 2	carbohydrate transport	1.3.55	0.3.88	1.0.56	0.7.14	
SLC25A5 protein	adenine transport	**0.3.87**	0.0.005	**0.4.28**	0.0.005	

The fold change of F2, F4 or F6 means that the protein abundance of three fractions is compared to fraction 1 of enterocytes and the column “Pval” means the *P* value.

© 1996-2016

Table 2. Increased abundances of proteins in the crypt compartment of jejunum of 21-day-old suckling piglets

Protein Name	Biological Process	Fold change (F2)	P val	Fold change (F4)	P val	Fold change (F6)
Annexin a2	developmental process	1.4.32	0.0.94	**3.2.50**	0.0.03	
Annexin A7	cell proliferation	0.8.24	0.9.73	0.8.09	0.6.60	
beta-tubulin	cytoskeleton-dependent intracellular transport	1.5.27	0.0.89	**2.2.90**	0.0.33	
ch4 and secrete domains of swine IgM	immune response	0.2.35	0.5.99	**3.4.99**	0.0.10	
Chain A, The Crystal Structure of Diferric Porcine Serum Transferrin	ferric iron binding	1.1.37	0.7.55	**3.0.47**	0.0.11	
Chain A, Structure Of 14-3-3 Isoform Sigma In Complex With A C-Raf1 Peptide And A Stabilizing Small Molecule Fragment	positive regulation of cell growth	**16.2.92**	0.0.04	2.1.67	0.5.05	
galectin-3	cell differentiation	**2.0.89**	0.0.03	0.9.12	0.9.06	
hypothetical protein	organelle organization	2.0.51	0.2.06	4.5.70	<0.0.001	
heat shock protein 90 alpha	immune response	0.4.13	0.1.78	0.8.39	0.5.25	
integrin beta-1	cell adhesion	2.0.32	0.0.93	**2.5.58**	0.0.46	
interleukin-1 beta converting enzyme	innate immune response	1.0.09	0.9.70	**1.6.74**	0.2.18	
Ppk 98; a protein kinase	toll-like receptor signaling pathway	0.3.66	0.0.81	**1.5.13**	0.1.57	
PREDICTED: actinin, alpha 1-like isoform 1	cell junction organization	1.0.66	0.7.55	**1.3.93**	0.1.36	
PREDICTED: cadherin-17	cell adhesion	1.2.13	0.9.14	0.5.80	0.0.35	
PREDICTED: EH domain-containing protein 1	cholesterol homeostasis	**2.8.31**	0.0.14	1.3.30	0.8.30	
PREDICTED: LOW QUALITY PROTEIN: myristoylated alanine-rich C-kinase substrate-like	energy metabolic process	9.3.75	0.1.70	**24.2.10**	0.0.29	
PREDICTED: LOW QUALITY PROTEIN: brain-specific angiogenesis inhibitor 1-associated protein 2-like protein 1-like	positive regulation of actin filament polymerization	**2.2.69**	0.1.33	**5.3.95**	0.0.06	
PREDICTED: protein S100-A14-like isoform 2	apoptotic process	2.5.35	0.4.06	**3.3.11**	0.0.14	
Ras gtpase-activating protein-binding protein 1	negative regulation of canonical Wnt receptor signaling pathway	**1.3.93**	0.0.14	**2.3.33**	0.0.07	
transferrin receptor protein 1	cellular iron ion homeostasis	0.7.51	0.9.87	5.1.05	0.0.76	
tropomyosin 5	cytoskeleton-dependent intracellular transport	1.8.03	0.0.92	**2.2.28**	0.0.35	
unnamed protein product	protein folding	0.8.55	0.6.01	**1.0.28**	0.8.26	
PREDICTED: 5'-AMP-activated protein kinase catalytic subunit alpha-1-like	catabolic process	**1.9.76**	0.0.41	0.8.87	0.0.51	
PREDICTED: major vault protein isoform 1	cell proliferation	0.9.63	0.8.41	1.1.06	0.9.69	
PREDICTED: neuroblast differentiation-associated protein AHNAK-like	nervous system development	0.5.75	0.2.63	0.7.11	0.4.84	
The fold change of F2, F4 or F6 means that the protein abundance of three fractions is compared to fraction 1 of enterocytes and the column "Pval" means the *P* value.						

of human nutrition and medicine, because the porcine, rather than the rodent, gastrointestinal tract is much closer to humans. In the present study, we performed an iTRAQ proteome analysis to identify jejunal BBM proteins that exhibited differential expression during the maturation of enterocytes in 21-day-old suckling piglets.

© 1996-2016

Table 3. The list of the identified proteins in the four fractions of jejunum of 21-day-old suckling piglets

Accession	Description	Peptides	Cov%	Fold change F2	P val	EF	Fold change F4	P val	EF	Fold change F6	P val	EF
gi|75075711	Adenylyl cyclase-associated protein 1	3	13.8.90	0.8.87	0.9.85	2.4.21	0.8.87	0.8.07	1.9.77	0.8.95	0.8.85	1.7.70
gi|62208269	ADP-ribosylation factor family-like protein	4	24.4.40	0.4.09	0.0.55	2.0.14	0.5.65	0.2.13	2.0.89	0.7.66	0.3.97	2.0.89
gi|51858555	Aldob protein	14	27.4.70	1.5.42	0.5.51	1.4.72	0.7.80	0.3.78	1.4.45	0.7.05	0.4.05	1.5.28
gi|87196501	alpha-enolase	13	37.3.30	1.2.25	0.2.92	1.3.80	1.1.07	0.4.44	1.3.80	1.1.27	0.4.88	1.3.80
gi|525287	aminopeptidase N	103	54.8.30	0.9.91	0.8.14	1.1.17	0.5.11	<0.0.001	1.3.30	0.0.82	<0.0.001	4.0.93
gi|178056703	angiotensin-converting enzyme 2	24	35.7.80	0.9.46	0.6.27	1.2.36	0.4.13	<0.0.001	1.5.70	0.0.86	<0.0.001	4.2.07
gi|145279215	angiotensin-converting enzyme isoform 2	25	23.4.50	1.6.60	0.0.26	1.3.55	0.7.18	0.3.07	1.3.18	0.0.68	<0.0.001	4.0.55
gi|54020966	annexin A2	23	58.4.10	1.4.32	0.0.94	1.3.30	3.2.51	0.0.04	2.1.88	3.8.02	<0.0.001	2.1.88
gi|94534942	Annexin A7	2	5.8.32	0.8.24	0.9.74	1.9.95	0.8.09	0.6.60	1.9.41	2.2.08	0.0.40	1.4.19
gi|262527580	AP-2 complex subunit alpha-1	7	9.8.26	0.9.38	0.5.77	1.2.02	0.9.91	0.6.46	1.1.80	0.9.64	0.9.21	1.2.02
gi|164359	apolipoprotein A-I	13	52.4.50	0.9.38	0.3.14	1.1.48	0.9.91	0.7.00	1.1.38	0.9.29	0.3.24	1.1.27
gi|47523830	apolipoprotein A-IV precursor	15	45.2.90	0.8.32	0.0.55	1.2.47	0.8.71	0.2.42	1.2.36	0.1.60	0.0.00	2.6.55
gi|178056175	basigin	4	14.8.70	1.3.93	0.3.50	1.4.32	1.1.48	0.1.69	1.4.59	1.7.86	0.3.15	1.4.72
gi|47522782	beta-2-microglobulin precursor	4	10.1.70	1.0.38	0.9.91	1.5.00	1.0.28	0.9.57	1.4.06	1.2.59	0.4.87	1.2.47
gi|90960962	beta-tubulin	26	49.1.00	1.5.28	0.0.89	1.7.22	2.2.91	0.0.33	1.8.71	2.5.35	0.0.13	1.9.05
gi|251823933	cadherin-1	4	5.7.76	0.9.38	0.8.82	1.3.30	0.9.29	0.5.98	1.2.36	0.9.91	0.8.41	1.2.82
gi|300798621	calcineurin B homologous protein 2	5	32.1.40	0.8.47	0.5.24	1.7.22	0.5.01	0.0.75	1.9.23	0.4.79	0.0.65	1.9.05
gi|329664002	calcium-activated chloride channel regulator 1	2	3.4.10	0.4.53	0.4.08	3.1.62	1.6.60	0.4.45	2.7.04	2.2.28	0.0.93	2.0.70
gi|223872	calmodulin	18	65.5.40	1.1.91	0.8.27	1.4.45	0.9.64	0.5.94	1.4.19	0.3.66	0.3.36	1.7.38
gi|291622246	calreticulin	4	13.6.70	0.5.40	0.1.59	1.6.75	1.6.00	0.1.78	1.5.42	1.7.22	0.0.62	1.5.85
gi|54035961	Caspase-3	9	31.4.10	1.1.69	0.8.42	1.4.86	1.1.48	0.9.62	1.5.28	0.5.92	0.2.20	1.6.44
gi|223634463	CD82 antigen	2	4.8.87	1.3.93	0.4.37	1.6.60	1.1.59	0.6.76	2.3.12	1.2.13	0.5.63	1.5.00
gi|78369384	cell surface A33 antigen	3	8.4.64	0.9.82	0.8.66	1.3.06	0.9.64	0.6.83	1.2.59	0.9.64	0.7.08	1.2.71
gi|1236646	ch4 and secrete domains of swine IgM	4	14.5.10	0.2.36	0.6.00	1.6.44	3.4.99	0.0.11	1.8.37	3.8.73	0.0.14	1.8.37
gi|75766221	Chain A, Crystal Structure Of A Soluble Form Of Clic4. Intercellular Chloride Ion Channel	4	20.2.20	0.8.32	0.4.00	1.5.85	0.8.39	0.4.99	1.6.14	0.7.31	0.1.55	1.4.86
gi|281500757	Chain A, Porcine Aldehyde Reductase In Ternary Complex With Inhibitor	4	18.7.70	0.8.63	0.1.75	1.2.02	0.8.39	0.0.99	1.2.02	0.9.73	0.8.97	1.3.06

(***Contd***...)

© 1996-2016

Table 3. (*Continued*)

Accession	Description	Peptides	Cov%	Fold change F2	P val	EF	Fold change F4	P val	EF	Fold change F6	P val	EF
gi|307776567	Chain A, Structure Of 14-3-3 Isoform Sigma In Complex With A C-Raf1 Peptide And A Stabilizing Small Molecule Fragment	3	15.9.00	16.2.93	0.0.04	2.6.55	2.1.68	0.5.06	2.1.48	1.2.71	0.8.56	2.9.11
gi|18655907	Chain A, The Crystal Structure Of Diferric Porcine Serum Transferrin	5	7.6.15	1.1.38	0.7.56	1.5.28	3.0.48	0.0.11	1.9.95	3.6.64	0.0.02	1.9.77
gi|198443144	Chain B, Crystal Structure Of Mammalian Fatty Acid Synthase In Complex With Nadp	5	2.9.06	2.4.89	0.4.40	2.2.08	5.4.45	0.2.79	2.1.88	4.5.29	0.2.03	2.2.08
gi|312062805	chloride intracellular channel protein 5	9	43.2.50	0.7.24	0.0.50	1.4.86	0.3.98	0.0.09	1.7.54	0.2.17	0.0.01	2.2.49
gi|227121291	claudin 3 variant 1	3	15.3.80	0.9.38	0.6.14	1.3.06	1.0.96	0.6.61	1.4.72	1.2.47	0.1.83	1.3.18
gi|223635227	Constitutive coactivator of PPAR-gamma-like protein 1	2	2.1.54	1.2.94	0.3.35	1.4.32	0.9.73	0.9.91	1.6.75	1.2.71	0.6.46	1.9.23
gi|190360617	cytochrome b reductase 1	9	18.2.50	0.4.29	0.5.03	1.5.14	0.3.47	0.2.99	1.4.72	0.0.74	0.1.73	2.9.11
gi|224176124	DEAD box polypeptide 58	3	4.8.78	1.0.28	0.7.20	1.3.06	0.9.38	0.7.81	1.4.19	0.9.91	0.9.57	1.4.19
gi|77736327	developmentally-regulated GTP-binding protein 1	2	8.1.74	0.3.50	0.2.29	2.0.89	1.4.45	0.5.14	2.1.09	1.4.32	0.5.17	2.0.89
gi|7939586	dihydrolipoamide succinyltransferase	2	3.9.56	0.4.21	0.2.45	2.6.79	0.3.50	0.2.00	1.7.70	0.5.65	0.3.78	2.1.68
gi|47523024	dipeptidase 1 precursor	5	14.1.80	1.1.59	0.4.82	1.5.14	0.6.49	0.1.09	1.4.72	0.4.37	0.0.17	1.5.42
gi|52001458	Dipeptidyl peptidase 4	10	14.7.50	0.6.92	0.0.81	1.3.68	0.5.15	0.0.00	1.4.72	0.1.66	0.0.00	3.1.05
gi|300669637	Epiplakin	4	4.2.44	3.8.73	0.0.97	1.7.22	0.6.14	0.1.76	1.6.75	0.0.71	0.1.45	1.7.38
gi|75045149	Epithelial cell adhesion molecule	7	18.7.90	1.4.32	0.7.86	1.5.14	1.6.29	0.4.25	1.5.42	2.0.32	0.1.81	1.6.60
gi|86450155	EPLIN-b	10	17.8.60	1.0.96	0.7.75	1.2.82	1.5.85	0.1.08	1.3.68	0.5.01	0.0.54	1.5.85
gi|148613357	F-actin capping protein alpha 1 subunit	8	38.8.10	0.9.91	0.5.66	1.3.30	1.0.67	0.2.38	1.2.36	0.9.38	0.9.69	1.2.82
gi|115503724	F-actin-capping protein subunit alpha-2	5	19.5.80	1.0.67	0.8.98	13.8.04	1.1.80	0.7.53	9.6.38	1.2.36	0.6.72	2.1.09
gi|91206621	Fatty acid-binding protein, intestinal	9	31.0.60	1.4.19	0.1.84	1.3.18	0.5.25	0.3.78	1.4.72	0.1.20	0.0.38	2.7.80
gi|300794998	filamin-B	18	8.9.63	0.9.55	0.9.20	1.4.32	0.4.92	0.2.73	3.6.31	0.9.12	0.7.71	4.4.46
gi|148230268	galectin-3	18	36.9.20	2.0.89	0.0.03	1.4.59	0.9.12	0.9.07	1.3.80	0.1.14	0.0.58	4.5.29
gi|218664463	galectin-8	2	11.6.70	0.3.87	0.2.51	2.0.89	0.9.73	0.9.68	2.0.89	0.1.04	0.1.11	2.1.09
gi|47523720	glucose-6-phosphate isomerase	16	26.7.00	1.4.06	0.1.00	1.3.93	0.6.61	0.5.72	1.4.45	0.7.31	0.5.95	1.4.06
gi|47523822	glutamate carboxypeptidase 2	7	10.1.20	0.9.04	0.4.17	1.1.48	0.9.82	0.5.40	1.1.27	0.9.55	0.6.65	1.1.27

(***Contd***...)

© 1996-2016

Table 3. (*Continued*)

Accession	Description	Peptides	Cov%	Fold change F2	P val	EF	Fold change F4	P val	EF	Fold change F6	P val	EF
gi|51701269	Glutamyl aminopeptidase	44	39.1.70	0.8.63	0.5.58	1.2.02	0.4.53	0.0.00	1.4.19	0.2.19	0.0.00	2.1.09
gi|296475036	glycerol-3-phosphate dehydrogenase 1-like protein	3	10.8.30	1.0.09	0.9.13	1.4.32	0.4.92	0.0.49	1.7.22	0.3.70	0.0.20	1.8.03
gi|81892782	Guanine nucleotide-binding protein G (s) subunit alpha isoforms Xlas	6	6.0.90	0.9.38	0.8.53	1.2.13	0.9.64	0.7.83	1.1.80	0.9.29	0.8.45	1.2.13
gi|217039113	HDL binding protein	9	10.6.80	1.2.13	0.7.10	1.4.06	1.5.56	0.1.24	1.4.86	0.7.31	0.3.26	1.4.59
gi|12082136	heat shock protein 90 alpha	29	32.2.70	0.4.13	0.1.78	1.7.06	0.8.39	0.5.25	1.2.71	2.7.04	0.0.01	1.5.70
gi|77736071	heterogeneous nuclear ribonucleoprotein K	11	26.5.10	0.6.98	0.1.81	1.3.06	2.3.99	0.2.57	1.7.86	2.5.59	0.0.47	1.5.14
gi|34364629	hypothetical protein	37	21.3.70	2.0.51	0.2.06	1.5.85	4.5.71	0.0.00	1.9.23	6.3.10	<0.0.001	1.9.95
gi|75050024	Integrin beta-1	5	7.2.68	2.0.32	0.0.94	1.7.86	2.5.59	0.0.46	1.9.05	2.9.38	0.0.25	1.9.41
gi|296490647	integrin, alpha 6	2	2.3.30	2.6.55	0.0.60	2.0.89	2.9.65	0.1.09	2.9.92	2.8.58	0.2.75	3.0.76
gi|6714562	interleukin-1 beta converting enzyme	3	8.9.11	1.0.09	0.9.71	1.8.03	1.6.75	0.2.19	1.8.88	2.3.33	0.0.18	1.7.06
gi|75054313	Junction plakoglobin	11	21.4.80	1.8.03	0.1.53	1.6.75	0.6.31	0.1.03	1.4.86	0.8.47	0.2.96	1.4.59
gi|190360611	junctional adhesion molecule A	3	16.4.40	1.1.38	0.7.07	4.0.18	0.9.55	0.9.21	4.6.99	0.8.87	0.7.70	4.0.18
gi|55956899	keratin, type I cytoskeletal 9	28	50.8.80	0.7.94	0.0.14	1.2.02	0.0.64	<0.0.001	2.0.89	0.0.45	<0.0.001	2.2.91
gi|623346	L-36 lactose binding protein	36	68.4.20	2.2.28	0.3.95	1.7.86	2.3.99	0.2.67	1.9.05	2.4.43	0.0.62	1.7.38
gi|71122452	LIM and SH3 protein 1	7	28.5.20	0.8.79	0.8.40	1.4.59	0.5.92	0.3.78	1.6.90	0.4.25	0.1.34	1.5.14
gi|75491026	liver fatty acid binding protein	22	75.5.90	1.5.28	0.7.17	2.2.08	0.3.02	0.5.04	2.6.55	0.1.19	0.2.93	3.1.62
gi|58332862	lysosome-associated membrane glycoprotein 1	2	5.8.11	0.9.20	0.6.97	1.4.59	1.0.76	0.6.99	1.8.37	1.0.47	0.7.08	1.6.75
gi|5739517	macrophage migration inhibitory factor	2	27.0.30	1.4.72	0.5.13	2.1.09	1.3.43	0.6.26	5.9.70	1.3.55	0.5.27	4.2.07
gi|148681621	mCG142196	9	9.2.05	0.7.59	0.5.86	2.1.48	0.5.01	0.2.95	2.0.89	0.2.56	0.1.46	2.0.89
gi|6647580	Membrane-associated progesterone receptor component 1	5	40.2.10	0.5.20	0.4.93	2.1.68	1.6.14	0.9.75	2.1.48	0.4.25	0.1.86	2.3.33
gi|75039721	Myosin-VI	17	14.9.90	0.9.55	0.3.24	1.3.06	0.8.63	0.1.46	1.2.02	0.8.02	0.0.58	1.3.30
gi|164382	Na+, K+-ATPase alpha-subunit precursor	59	39.0.80	1.0.00	0.2.92	1.2.25	0.6.49	0.0.02	1.2.47	0.3.19	<0.0.001	1.8.54
gi|47523762	plasma membrane calcium-transporting ATPase 1	16	16.6.40	1.5.42	0.3.29	2.4.21	1.2.71	0.5.14	20.8.93	0.9.29	0.9.02	19.2.31
gi|40849918	plectin 6	9	1.8.57	0.7.59	0.4.03	1.9.05	0.7.73	0.3.32	1.5.56	0.9.04	0.8.38	1.6.14

(***Contd***...)

© 1996-2016

Table 3. (*Continued*)

Accession	Description	Peptides	Cov%	Fold change F2	P val	EF	Fold change F4	P val	EF	Fold change F6	P val	EF
gi|6863080	poly-Ig receptor	4	8.8.39	1.9.77	0.7.14	2.2.91	2.8.58	0.5.25	2.1.68	3.0.48	0.1.09	2.2.49
gi|431944	Ppk 98; a protein kinase	23	31.2.20	0.3.66	0.0.82	1.8.20	1.5.14	0.1.58	1.2.47	2.9.38	0.0.01	1.5.42
gi|335297640	PREDICTED: 2',3'-cyclic-nucleotide 3'-phosphodiesterase	2	7.3.81	1.1.48	0.6.06	1.5.00	1.1.48	0.5.82	2.1.88	0.9.64	0.9.42	1.8.71
gi|335281655	PREDICTED: 4F2 cell-surface antigen heavy chain	10	23.4.50	1.1.91	0.6.36	1.2.71	0.7.52	0.7.23	1.3.80	0.3.44	0.0.08	1.8.71
gi|311277261	PREDICTED: 55 kDa erythrocyte membrane protein-like isoform 1	7	18.8.80	0.8.39	0.9.17	1.4.86	0.5.97	0.1.06	1.4.59	0.4.33	0.1.97	1.8.37
gi|296194720	PREDICTED: 5'-AMP-activated protein kinase catalytic subunit alpha-1-like	2	3.9.95	1.9.77	0.0.42	4.2.07	0.8.87	0.0.52	4.4.46	1.7.06	0.0.45	4.4.06
gi|311258794	PREDICTED: acid sphingomyelinase-like phosphodiesterase 3b	16	36.3.60	0.7.94	0.3.07	1.2.71	0.3.25	0.0.00	1.6.60	0.2.58	<0.0.001	1.7.86
gi|291406471	PREDICTED: actinin, alpha 1-like isoform 1	17	17.9.40	1.0.67	0.7.56	1.4.19	1.3.93	0.1.37	1.4.72	2.7.29	0.0.03	1.7.38
gi|291409670	PREDICTED: adenosine deaminase	5	12.0.10	0.6.67	0.4.97	2.0.89	0.5.86	0.4.08	2.0.89	0.4.17	0.2.70	2.0.89
gi|291392546	PREDICTED: ADP-ribosylation factor 1	6	32.0.40	1.1.27	0.9.64	1.5.14	0.9.82	0.4.97	1.5.00	1.7.86	0.6.75	1.6.75
gi|296206637	PREDICTED: alpha-enolase isoform 1	12	36.8.70	0.7.45	0.6.03	2.1.09	0.6.25	0.4.47	2.0.89	0.6.79	0.5.15	2.1.09
gi|301791379	PREDICTED: angiotensin-converting enzyme 2-like	4	4.5.96	0.4.57	0.5.33	2.7.80	0.3.37	0.4.05	2.1.09	0.2.38	0.3.07	1.8.03
gi|311251426	PREDICTED: ankyrin repeat and SAM domain-containing protein 4B	3	9.1.13	0.5.65	0.1.44	1.6.44	0.6.67	0.1.66	1.4.59	0.4.57	0.0.19	1.6.29
gi|334324681	PREDICTED: AP-1 complex subunit beta-1-like	8	11.5.60	0.8.63	0.3.61	1.6.90	1.0.47	0.9.37	1.4.72	0.9.91	0.3.53	1.7.06
gi|332208296	PREDICTED: apolipoprotein A-I-like isoform 4	2	10.8.60	0.5.70	0.1.90	1.5.00	0.4.61	0.1.02	2.0.89	0.6.61	0.2.15	2.0.32
gi|301778975	PREDICTED: band 4.1.-like protein 3-like	6	7.4.45	0.6.61	0.4.87	2.0.89	1.0.57	0.9.00	2.0.89	1.0.00	0.9.80	2.0.89
gi|335306675	PREDICTED: b-cell receptor-associated protein 31-like	2	7.7.24	0.9.73	0.8.71	1.4.86	1.2.94	0.1.58	1.3.80	1.0.57	0.6.12	1.5.42
gi|194037042	PREDICTED: cadherin-17	7	6.6.11	1.2.13	0.9.14	1.5.00	0.5.81	0.0.36	1.6.75	0.4.79	0.1.24	1.7.54

(***Contd***...)

© 1996-2016

Table 3. (*Continued*)

Accession	Description	Peptides	Cov%	Fold change F2	P val	EF	Fold change F4	P val	EF	Fold change F6	P val	EF
gi|194037042	PREDICTED: cadherin-17 (Sus scrofa)	7		1.2.13	0.9.14	1.5.00	0.5.81	0.0.36	1.6.75	0.4.79	0.1.24	1.7.54
gi|114675715	PREDICTED: cAMP-dependent protein kinase catalytic subunit alpha isoform 2	2	6.7.92	1.0.19	0.9.43	19.0.55	0.8.09	0.6.86	20.5.12	0.3.47	0.2.20	28.0.54
gi|194041842	PREDICTED: canalicular multispecific organic anion transporter 1	8	7.7.77	0.9.20	0.3.55	1.3.18	0.6.67	0.0.07	1.3.55	0.3.13	<0.0.001	1.8.37
gi|126340910	PREDICTED: cationic trypsin-3-like	5	7.6.92	0.8.95	0.8.36	2.0.89	1.0.28	0.9.39	2.0.89	0.6.37	0.4.58	2.0.89
gi|311247985	PREDICTED: CD44 antigen-like isoform 2	2	3.8.36	1.4.19	0.5.29	2.0.89	12.9.42	0.0.96	2.1.28	20.1.37	0.0.83	2.1.48
gi|311254317	PREDICTED: cingulin-like	9	8.4.45	1.0.19	0.7.12	1.1.69	1.1.27	0.2.85	1.1.69	1.0.38	0.6.44	1.1.38
gi|334346971	PREDICTED: cytoplasmic FMR1-interacting protein 1-like isoform 2	3	2.6.38	0.9.55	0.4.26	1.2.59	1.0.09	0.8.54	1.2.36	1.0.67	0.6.61	1.2.36
gi|109486899	PREDICTED: dipeptidyl-peptidase 3-like	2	2.9.81	0.9.82	0.7.49	1.8.88	0.8.95	0.6.57	2.2.70	1.4.06	0.6.02	1.8.20
gi|311275781	PREDICTED: drebrin-like protein-like	4	11.5.00	0.8.63	0.4.49	1.8.71	0.8.71	0.5.83	1.5.00	0.8.95	0.5.18	1.5.14
gi|335281293	PREDICTED: ectonucleoside triphosphate diphosphohydrolase 8-like	4	9.8.99	0.9.91	0.9.92	4.3.25	0.6.43	0.2.95	1.6.44	0.2.68	0.0.76	5.1.05
gi|335281552	PREDICTED: EH domain-containing protein 1	7	14.9.80	2.8.31	0.0.15	1.8.37	1.3.30	0.8.30	1.4.86	0.5.86	0.3.92	1.6.60
gi|311258366	PREDICTED: espin	2	1.8.71	0.8.55	0.7.70	2.7.29	0.7.66	0.4.80	1.5.85	0.0.98	0.0.75	4.4.46
gi|194042010	PREDICTED: gamma-adducin isoform 1	2	3.6.83	0.7.38	0.3.13	4.1.69	0.8.87	0.6.93	4.3.65	1.4.45	0.2.27	4.0.93
gi|301764284	PREDICTED: glutamyl aminopeptidase-like	16	15.2.30	0.3.73	0.2.43	2.1.09	0.5.11	0.3.39	2.0.89	0.4.45	0.2.89	2.0.89
gi|332237751	PREDICTED: GTPase NRas-like	2	9.4.59	1.1.17	0.7.20	14.4.54	0.7.94	0.5.18	20.5.12	0.6.55	0.3.30	2.2.49
gi|335297447	PREDICTED: guanine nucleotide-binding protein subunit alpha-13	5	19.3.60	1.0.57	0.8.48	1.4.06	1.0.96	0.4.52	1.6.14	0.9.29	0.7.15	1.5.14
gi|291400199	PREDICTED: heat shock 70kDa protein 8	32	47.9.90	0.8.87	0.4.14	1.8.71	0.9.04	0.5.21	1.9.23	1.0.19	0.7.49	1.5.42
gi|335284210	PREDICTED: heat shock protein beta-1-like isoform 1	5	25.6.50	1.1.38	0.4.55	1.5.42	1.0.38	0.7.47	1.3.55	1.0.96	0.5.51	1.4.86
gi|334348624	PREDICTED: hypothetical protein LOC100009833	13	5.1.44	1.0.38	0.9.67	1.6.90	0.7.59	0.3.62	1.4.72	0.7.52	0.2.69	1.4.86

(***Contd***...)

© 1996-2016

Table 3. (*Continued*)

Accession	Description	Peptides	Cov%	Fold change F2	P val	EF	Fold change F4	P val	EF	Fold change F6	P val	EF
gi|334313835	PREDICTED: hypothetical protein LOC100019323	2	2.5.94	0.9.82	0.2.28	1.3.43	1.0.09	0.2.90	1.2.59	1.0.47	0.4.06	1.3.30
gi|311273235	PREDICTED: intestinal-type alkaline phosphatase-like isoform 2	26	45.0.30	0.6.19	0.0.10	1.3.68	0.6.08	0.0.05	1.3.43	0.3.94	0.0.00	1.5.70
gi|301782399	PREDICTED: leukocyte surface antigen CD47-like, partial	2	4.9.35	1.2.02	0.7.11	2.0.89	0.6.61	0.4.89	2.0.89	1.3.43	0.5.81	2.0.89
gi|335284027	PREDICTED: LOW QUALITY PROTEIN: brain-specific angiogenesis inhibitor 1-associated protein 2-like protein 1-like	5	14.5.40	2.2.70	0.1.34	1.9.23	5.3.95	0.0.07	2.9.65	4.6.13	0.0.18	2.6.55
gi|338715029	PREDICTED: LOW QUALITY PROTEIN: cytoplasmic dynein 1 light intermediate chain 1-like	2	5.9.16	0.7.59	0.5.54	1.6.00	0.6.85	0.5.65	4.4.46	0.6.79	0.4.30	1.6.00
gi|335281047	PREDICTED: LOW QUALITY PROTEIN: long-chain fatty acid transport protein 4	5	10.3.60	1.2.25	0.8.65	1.7.70	1.0.28	0.6.45	1.7.22	0.4.74	0.3.06	1.8.37
gi|335279372	PREDICTED: LOW QUALITY PROTEIN: myristoylated alanine-rich C-kinase substrate-like	2	10.5.40	9.3.76	0.1.71	6.4.27	24.2.10	0.0.30	5.8.61	29.1.07	0.0.30	5.4.45
gi|334333162	PREDICTED: LOW QUALITY PROTEIN: talin-1-like	5	2.4.80	1.1.17	0.4.01	1.4.32	1.1.17	0.3.11	1.3.68	1.1.69	0.2.59	1.4.45
gi|335284397	PREDICTED: major vault protein isoform 1	14	23.8.90	0.9.64	0.8.42	1.3.06	1.1.07	0.9.69	1.3.18	1.8.37	0.0.03	1.4.06
gi|149747264	PREDICTED: maltase-glucoamylase, intestinal	19	10.4.50	1.6.00	0.1.81	4.4.46	0.4.97	0.5.12	4.0.93	0.4.45	0.2.06	4.4.87
gi|301772598	PREDICTED: maltase-glucoamylase, intestinal-like	12	6.4.76	1.3.06	0.6.28	2.4.21	0.2.27	0.5.87	3.4.67	0.0.83	0.2.36	5.5.46
gi|311259100	PREDICTED: meprin A subunit beta	9	16.9.80	1.3.18	0.0.85	1.3.80	0.5.65	0.0.44	1.4.72	0.2.07	0.0.01	2.2.49
gi|297298984	PREDICTED: microtubule-associated tumor suppressor 1 homolog	2	1.9.05	1.0.86	0.7.95	2.3.77	1.2.94	0.5.00	2.0.51	1.1.27	0.7.38	1.8.54
gi|311254039	PREDICTED: mucosal pentraxin-like	4	24.6.60	0.1.98	0.1.43	3.2.81	0.8.63	0.7.89	1.4.86	1.5.85	0.2.90	1.6.60
gi|335295539	PREDICTED: multidrug resistance protein 1 isoform 2	18	17.8.80	0.7.66	0.0.79	1.2.25	0.3.87	0.0.00	1.5.00	0.1.24	0.0.00	3.0.48

(***Contd***...)

© 1996-2016

Table 3. (*Continued*)

Accession	Description	Peptides	Cov%	Fold change F2	P val	EF	Fold change F4	P val	EF	Fold change F6	P val	EF
gi|301784356	PREDICTED: myosin regulatory light polypeptide 9-like	7	15.7.10	1.6.60	0.0.57	1.4.72	0.7.38	0.4.65	1.5.42	0.7.52	0.5.13	1.5.00
gi|291391371	PREDICTED: myosin VIIB-like	5	2.6.02	1.2.94	0.5.23	7.7.27	0.7.31	0.5.62	21.0.86	1.7.54	0.2.73	20.5.12
gi|311264064	PREDICTED: Na(+)/H(+) exchange regulatory cofactor NHE-RF4 isoform 1	2	5.9.29	0.7.66	0.5.71	1.8.37	0.9.12	0.8.40	1.3.80	0.8.55	0.6.51	3.1.62
gi|311247353	PREDICTED: n-acetylated-alpha-linked acidic dipeptidase-like protein	17	23.9.90	1.0.47	0.9.17	1.3.93	0.4.25	0.0.00	1.6.44	0.2.44	0.0.00	2.2.91
gi|311250752	PREDICTED: NACHT, LRR and PYD domains-containing protein 6	2	3.1.04	0.8.87	0.3.62	1.3.18	0.9.38	0.6.60	1.3.55	1.0.09	0.9.49	1.5.56
gi|297267662	PREDICTED: neuroblast differentiation-associated protein AHNAK-like	9	7.1.20	0.5.75	0.2.63	2.2.49	0.7.11	0.4.85	2.2.70	1.8.54	0.0.39	1.7.06
gi|291406817	PREDICTED: numb homolog isoform 4	2	3.1.15	0.9.73	0.8.92	1.4.59	0.8.09	0.2.55	1.6.00	0.8.24	0.3.52	1.5.70
gi|109098176	PREDICTED: plasma membrane calcium-transporting ATPase 1-like isoform 3	16	15.1.70	1.0.38	0.9.63	8.3.95	1.0.76	0.8.82	2.0.89	0.9.20	0.8.49	3.0.48
gi|332809366	PREDICTED: plasminogen activator inhibitor 1 RNA-binding protein isoform 3	3	8.6.67	5.1.05	0.1.95	2.7.04	22.9.09	0.0.71	3.9.08	12.5.89	0.1.15	3.4.99
gi|301773440	PREDICTED: plectin-1-like	6	1.5.57	1.4.19	0.4.57	2.0.89	1.1.38	0.7.82	19.9.53	1.3.18	0.5.21	3.0.20
gi|335308997	PREDICTED: probable phospholipid-transporting ATPase IC	4	3.6.71	1.3.43	0.1.75	1.5.00	0.7.38	0.4.93	1.5.14	0.8.39	0.4.90	1.5.56
gi|334322499	PREDICTED: protein S100-A14-like isoform 2	4	37.5.00	2.5.35	0.4.07	2.5.12	3.3.11	0.0.15	2.6.06	13.0.62	0.0.04	3.6.64
gi|311274096	PREDICTED: proton-coupled amino acid transporter 1	2	8.8.24	1.2.36	0.6.71	2.0.89	0.6.03	0.4.24	2.0.89	0.6.79	0.5.09	2.0.89
gi|194038728	PREDICTED: pyruvate kinase isozymes M1/M2 isoform 1	21	44.4.40	0.8.95	0.7.73	1.2.13	0.4.92	0.0.01	1.4.86	0.7.05	0.0.63	1.2.82
gi|334332964	PREDICTED: ras-related C3 botulinum toxin substrate 1-like	2	7.2.89	0.5.70	0.1.21	2.0.51	0.5.70	0.1.07	1.7.06	0.4.61	0.1.14	1.9.95

(***Contd***...)

© 1996-2016

Table 3. (*Continued*)

Accession	Description	Peptides	Cov%	Fold change F2	P val	EF	Fold change F4	P val	EF	Fold change F6	P val	EF
gi|332215306	PREDICTED: ras-related protein Rab-5A-like isoform 2	2	11.4.40	1.6.75	0.3.67	2.9.65	1.2.36	0.4.32	20.7.01	1.3.93	0.4.69	7.8.70
gi|296238536	PREDICTED: ras-related protein R-Ras2-like	5	28.4.30	1.5.14	0.2.31	4.2.07	1.0.76	0.5.05	3.6.98	0.7.05	0.2.73	4.0.18
gi|297262660	PREDICTED: receptor tyrosine-protein kinase erbB-3 isoform 4	3	2.4.15	1.0.47	0.6.94	1.9.95	1.3.80	0.1.59	1.5.14	1.4.32	0.0.90	1.5.70
gi|73988219	PREDICTED: similar to Rho-related GTP-binding protein RhoG (Sid 10750)	3	16.4.70	1.0.38	0.5.80	1.2.13	0.9.55	0.5.38	1.1.91	0.9.29	0.4.17	1.2.13
gi|311248065	PREDICTED: sodium-coupled monocarboxylate transporter 2-like	3	6.3.00	1.1.91	0.4.66	1.3.93	0.5.15	0.0.55	1.3.43	0.1.14	0.0.14	4.0.18
gi|335304268	PREDICTED: sodium-dependent neutral amino acid transporter B (0) AT1	8	8.9.91	1.2.71	0.5.29	1.4.32	0.5.70	0.0.96	1.6.90	0.2.25	0.0.62	2.3.33
gi|311268673	PREDICTED: solute carrier family 22 member 13	4	6.9.97	0.8.17	0.3.46	1.5.70	0.6.14	0.1.82	2.0.51	0.2.56	0.0.26	1.9.23
gi|335278852	PREDICTED: sorting nexin-9-like	2	4.3.77	0.8.87	0.7.57	3.7.67	0.6.85	0.5.52	2.5.82	0.5.25	0.3.22	3.4.36
gi|149756088	PREDICTED: sucrase-isomaltase, intestinal isoform 1	15	7.5.58	0.9.91	0.3.48	1.4.86	0.4.33	0.0.60	1.8.71	0.4.53	0.0.27	1.7.54
gi|311248566	PREDICTED: syntaxin-binding protein 2	8	15.1.80	1.0.96	0.7.79	3.1.33	0.6.43	0.3.16	2.7.54	0.3.98	0.1.68	8.8.72
gi|301779942	PREDICTED: t-complex protein 1 subunit alpha-like	9	19.4.20	0.8.79	0.3.99	1.4.86	1.0.28	0.8.14	1.5.28	1.1.48	0.3.14	1.1.80
gi|335294984	PREDICTED: trehalase	2	6.5.97	0.6.43	0.4.56	1.2.71	0.9.38	0.9.09	1.7.22	0.8.95	0.9.55	2.5.35
gi|311270318	PREDICTED: zinc transporter ZIP14	2	4.4.90	0.9.55	0.9.86	1.4.72	1.1.38	0.6.95	1.4.32	1.4.86	0.5.15	1.2.94
gi|304365428	protein disulfide-isomerase A3	18	40.9.90	0.3.53	0.0.08	1.8.54	1.1.27	0.8.23	1.2.59	1.2.47	0.8.28	1.2.94
gi|304365440	protein disulfide-isomerase A6	8	28.4.10	0.4.74	0.0.34	1.6.90	0.9.73	0.7.43	1.5.56	1.6.60	0.2.97	1.5.42
gi|296476109	protein disulfide-isomerase precursor	13	23.9.20	0.9.73	0.9.63	2.0.89	0.7.73	0.6.44	2.0.89	0.5.50	0.3.74	2.0.89
gi|55742801	protein S100-G	10	60.7.60	0.8.02	0.6.79	1.2.47	0.4.83	0.3.06	1.4.59	0.0.42	0.0.02	5.9.16
gi|75043802	Rab GDP dissociation inhibitor beta	5	14.6.10	1.0.00	0.4.56	1.0.96	1.0.38	0.1.98	1.1.07	0.9.82	0.7.61	1.1.17
gi|915	rab10	5	32.0.00	0.8.79	0.6.33	1.2.47	1.0.28	0.7.56	1.2.25	1.0.19	0.6.88	1.2.25

(***Contd***...)

© 1996-2016

Table 3. (*Continued*)

Accession	Description	Peptides	Cov%	Fold change F2	P val	EF	Fold change F4	P val	EF	Fold change F6	P val	EF
gi|14595132	Raichu404X	7	9.2.35	1.0.09	0.8.04	1.2.02	0.9.73	0.6.31	1.2.02	1.0.47	0.8.44	1.1.80
gi|329663948	ras GTPase-activating protein-binding protein 1	2	6.2.37	1.3.93	0.0.14	3.4.04	2.3.33	0.0.08	1.3.93	3.1.92	0.0.06	1.9.23
gi|85700392	Ras-related protein Rab-14	4	22.3.30	1.2.59	0.5.00	1.4.59	1.7.70	0.1.61	1.2.94	1.5.85	0.2.27	1.9.95
gi|16758202	ras-related protein Rab-27B	2	5.9.63	0.7.94	0.3.60	1.8.54	0.8.24	0.2.99	1.8.37	0.8.24	0.3.59	1.5.42
gi|77736431	ras-related protein Rab-5C	6	42.5.90	0.9.82	0.4.89	1.2.71	0.9.04	0.8.00	1.2.25	0.9.64	0.7.54	1.2.94
gi|84579874	ras-related protein R-Ras	3	17.8.90	1.0.67	0.6.06	8.2.41	0.8.87	0.5.83	3.9.08	0.8.39	0.3.92	5.4.95
gi|149041248	rCG27551, isoform CRA_a	3	20.4.20	0.7.73	0.3.37	2.0.89	0.8.02	0.3.59	5.2.97	0.7.24	0.2.77	2.1.09
gi|48474224	Scavenger receptor class B member 1	2	4.5.19	1.5.42	0.4.21	6.2.52	0.9.91	0.9.88	14.4.54	0.4.97	0.2.71	9.1.20
gi|95767522	SH3-domain GRB2-like 1	3	8.6.72	0.9.38	0.9.36	1.2.94	0.9.82	0.9.68	1.2.36	1.0.09	0.8.48	1.2.02
gi|6094365	Signal transducer and activator of transcription 2	2	4.0.51	0.2.81	0.1.92	2.1.09	0.2.36	0.1.69	2.0.89	0.2.23	0.1.64	2.1.09
gi|94471896	signal transducer and activator of transcription 3	5	10.0.00	0.8.71	0.6.66	2.1.88	0.8.02	0.3.81	1.5.85	0.7.66	0.3.17	1.8.54
gi|45829841	SLC25A5 protein	4	12.0.70	0.3.87	0.0.01	1.6.60	0.4.29	0.0.01	1.6.00	0.2.94	0.0.00	1.7.70
gi|255683521	sodium/glucose cotransporter 1	9	14.6.50	0.9.55	0.9.94	1.2.02	0.3.84	0.0.01	1.3.30	0.0.41	0.0.03	5.0.12
gi|148236169	solute carrier family 2, facilitated glucose transporter member 2	3	6.6.79	1.3.55	0.3.88	1.4.06	1.0.57	0.7.15	1.5.56	0.3.53	0.0.09	1.8.03
gi|298677090	superoxide dismutase	3	19.6.10	1.5.00	0.5.33	1.7.22	1.5.42	0.6.74	1.7.54	2.0.89	0.2.09	1.7.54
gi|75056777	Transferrin receptor protein 1	5	8.8.54	0.7.52	0.9.88	1.3.93	5.1.05	0.0.77	2.0.70	7.4.47	0.0.03	2.1.28
gi|20269390	TRK-fused gene/ anaplastic large cell lymphoma kinase extra long form	2	4.6.08	0.9.64	0.9.12	4.2.85	0.6.61	0.2.76	2.0.89	0.9.38	0.8.38	2.0.89
gi|9653293	tropomyosin 5	8	31.0.50	1.8.03	0.0.93	1.5.28	2.2.28	0.0.35	1.5.42	2.3.77	0.0.14	1.5.56
gi|78000201	tropomyosin alpha-1 chain isoform h	5	19.3.50	1.0.96	0.5.62	1.5.28	1.0.38	0.6.66	1.7.38	1.0.57	0.5.22	1.5.85
gi|20178270	Tropomyosin alpha-4 chain	8	31.0.50	1.0.09	0.9.17	1.3.18	0.9.82	0.8.74	1.2.94	1.1.07	0.4.09	1.3.06
gi|136429	Trypsin	56	51.0.80	0.3.47	0.3.60	1.4.59	0.3.77	0.3.43	1.4.72	0.7.18	0.7.21	1.2.71
gi|93140718	Tubulin beta-2C chain	25	46.2.90	1.1.07	0.1.85	1.5.14	1.0.00	0.7.47	1.3.68	1.0.57	0.8.43	1.5.85
gi|300652166	unnamed protein product	2	5.8.50	1.2.36	0.2.04	2.7.04	1.6.90	0.1.27	2.0.70	0.9.82	0.4.26	2.7.29
gi|90076980	unnamed protein product	6	31.0.90	1.0.47	0.5.37	1.2.71	1.0.86	0.9.40	1.3.43	1.1.27	0.7.11	1.4.72
gi|194384276	unnamed protein product	4	24.1.50	1.1.17	0.6.94	1.6.14	0.7.38	0.4.28	1.5.42	0.5.30	0.1.35	1.8.54
gi|40042562	unnamed protein product	5	23.7.10	1.0.86	0.7.49	1.3.43	1.0.96	0.6.72	1.3.55	1.4.59	0.0.83	1.3.43

(***Contd***...)

© 1996-2016

Table 3. (*Continued*)

Accession	Description	Peptides	Cov%	Fold change F2	P val	EF	Fold change F4	P val	EF	Fold change F6	P val	EF
gi|194389640	unnamed protein product	10	22.4.30	0.7.45	0.4.46	1.4.45	0.6.92	0.1.53	1.4.59	0.6.43	0.1.13	1.4.86
gi|74195800	unnamed protein product	5	14.1.00	0.8.95	0.6.45	1.1.80	0.8.95	0.1.51	1.1.59	0.8.95	0.3.80	1.1.91
gi|21336470	unnamed protein product	2	11.7.30	0.6.55	0.4.82	2.0.89	0.6.19	0.4.42	2.0.89	1.2.71	0.6.41	2.0.89
gi|90075818	unnamed protein product	23	26.1.00	0.8.55	0.6.02	1.3.80	1.0.28	0.8.27	1.4.19	2.1.28	0.0.37	1.5.42
gi|4995882	urate transporter/channel protein, isoform (UATp, i)	4	14.3.30	0.9.20	0.7.40	1.6.14	1.2.02	0.6.81	1.6.60	1.1.59	0.7.40	1.2.59
gi|86822282	Vesicle-associated membrane protein 3 (cellubrevin)	2	31.7.30	0.8.63	0.6.38	3.1.33	1.2.94	0.3.96	2.5.35	1.3.93	0.3.14	1.3.80
gi|7669550	vinculin isoform meta-VCL	7	8.3.77	1.0.57	0.6.98	1.2.13	0.9.73	0.5.52	1.2.13	1.0.86	0.3.82	1.2.13
gi|296480656	Yamaguchi sarcoma viral (v-yes-1) oncogene homolog isoform 2	6	13.2.80	0.7.94	0.6.31	2.2.08	1.2.71	0.6.12	2.2.08	2.1.68	0.1.47	2.2.08

The table lists the mass spectrometry data used for quantitative comparison of proteins, including the number of peptides, the coverage of each protein assigned, species, the protein abundance at fraction 2,4,6 compared to fraction 1, the *P* value, etc.In the “peptides” column, the values represent the number of peptides with 95% confidence. In the “Cov%” column, the values represent the coverage (%) of each protein assigned by the peptides. The “fold change F2 “, “fold change F4 “ and “fold change F6 “ means that the protein abundance in franction 2, 4 and 6 is compared to that in fraction 1 of suckling piglets. In the “Pval” column, the values represent the probability values by statistical analysis and the probability values<0.0.5 were used to indicate statistical significance.In the “EF” column, the values represent the error value of quantitative peptides

We found that digestive enzymes and transporters were predominantly down-regulated, and proteins related to signal transduction were upregulated along the crypt-villus axis.

Peptidases, enzymes present in the brush-border membrane and in the cytosol of enterocytes of the small intestine, are responsible for the hydrolysis of peptides into smaller peptides and amino acids. Three major oligopeptidases, including aminopeptidase N (APN), glutamyl aminopeptidase (aminopeptidase A, APA), and dipeptidyl peptidase 4 (DPP IV), were identified to be down-regulated in the crypt compartment from the BBM of the piglets. These oligopeptidases are involved in the final stage of protein digestion to generate free amino acids APA preferentially hydrolyses peptide bonds consisting of neutral and basic amino acids from the N-terminal end of oligopeptides (20), participates in localized immune responses in antigen presentation (21), and aids in the regulation of inflammatory responses (22). Na^+/K^+ -transporting ATPase (Na^+/K^+ ATPase) and sucrase-isomaltase exhibited reduced expression in the crypt compartment. Similarly, Goda *et al.* (23) reported that the expression of sucrose-isomaltase was higher in the villus than in the crypt (23). In neonatal pigs, Fan *et al.* (6) found that the activity of alkaline phosphatase, APN, Na^+/K^+ ATPase, and sucrase activities increased along the crypt-villus axis in both the proximal and distal small intestine. Results of the present study supported the view that the ability of nutrient digestion is enhanced when enterocytes differentiate along the crypt-villus axis in the small intestine of 21-day-old suckling piglets.

The intestinal tissues are capable of oxidizing three substrates for energy, including amino acids, glucose, and fatty acids. The suckling period is characterized by the abundance of lipids in milk, and proteins involved in fatty acid absorption play a prominent role in intestinal development. Several proteins (long-chain fatty acid transport protein 4, fatty acid binding protein 5 (FABP 5), intestinal fatty acid binding protein (I-FABP), and liver fatty acid binding protein (L-FABP)) with key roles in the absorption of fatty acids in the small intestine were identified in the present study.

Long-chain fatty acid transport protein 4, which had been suggested to play an important role in the uptake of long-chain fatty acids and to be the principal fatty acid transporter in enterocytes (24), remained constant along the crypt-villus axis. Fatty acid-binding proteins (FABPs) contribute to the transfer of absorbed fatty acids to the endoplasmic reticulum, where re-synthesis of complex lipids takes place. The two major isoforms of FABP found in enterocytes, the intestinal-type (I-FABP) and the liver-type (L-FABP), are known to have different binding specificities. These isoforms exhibited dissimilar expression profiles along the crypt-villus axis in the piglets. L-FABP levels remained constant

© 1996-2016

during enterocyte maturation in 21-day-old suckling piglets, whereas the expression of I-FABP increased in the crypt compartment. Previous studies showed that the metabolism of fatty acids in piglets was influenced by the presence of specific bacteria (25). In addition, the nutrient composition of the milk itself may change during lactation (26), which necessitates alterations in expression of digestive enzymes in the gastrointestinal tract.

In the present study, we identified four glucose transporters: sodium/glucose co-transporter 1, solute carrier family 2, facilitated glucose transporter member 2, and low affinity sodium-glucose co-transporter. The sodium/glucose co-transporter 1 was upregulated in the villus. Previous studies also have shown that the expression of glucose transporters (SGLT1 and GLUT5) and L-FABP is higher in the villus than the crypt (27-29). However, Yang *et al.* (30) demonstrated that the expression of SGLT1 is similar along the jejunal crypt-villus axis in neonatal piglets (30). This discrepancy may be due to the different growth stages. The findings of the present work suggest that the ability to absorb nutrients is altered when enterocytes differentiate along the crypt-villus axis in the small intestine of 21-day-old suckling piglets.

We identified 25 upregulated BBM proteins in the other three epithelial cell fractions compared to the villus tip, including the annexin family of Ca^{2+}-regulated membrane binding proteins, transferrin receptor proteins, and ion channels. In mice, transferrin receptors are localized to the small-intestinal absorptive cells (31). Annexin a2 and a7 are members of the annexin family of Ca^{2+}-regulated membrane binding proteins, which link to actin remodeling processes in cells (32) and may participate in membrane fusion processes (33). However, the expression profiles of these two proteins in piglet BBM were not consistent with those reported for Caco-2 cells (17). Chloride intracellular channel 5 was expressed at the highest abundance in the upper villus and showed a continuous decrease in the other three epithelial cell fractions. This channel plays an important role in maintaining the balance of water and electrolytes, regulating cell volume, and controlling the membrane potential (34).

The apical and basolateral membranes of enterocytes are separated by distinct, complex protein systems, including tight junctions, which regulate the paracellular permeability of intestinal epithelia. Cell-cell interactions are likely to play a role in the stem cell niche (35). Integrins are heterodimeric transmembrane glycoproteins composed of non-covalently linked alpha and beta subunits, which are endowned with both structural and regulatory functions. Our results revealed upregulation of integrin beta 1 in the middle villus and crypt regions, whereas the expression of integrin alpha 6 did not change in all the four fractions. Integrin alpha 6 is a subunit of two distinct glycoprotein complexes, where it combines with either integrin beta 1 or beta 4. As a result, the distribution of integrin alpha 6 corresponds more closely to that of integrin beta 4 than to the distribution of integrin beta 1 during intestinal development (36). A previous study showed that integrin-mediated functional polarization of Caco-2 cells occurs through E-cadherin-actin complexes (37), and the junctional adhesion molecule A (JAM-1) regulates epithelial cell morphology by affecting integrin beta-1 and Rap1 (38). In contrast, our findings indicate that the expression of these two proteins did not change in any of epithelial cell fractions examined. This reflects a difference bewteen cultured cells and the small intestine *in vivo*.

The permeability barrier of the brush-border in the small intestine is also characterized by a high content of glycolipids. Galectins, a family of animal lectins with conserved carbohydrate-recognition domains that bind β-galactosides, can regulate cell-surface glycoprotein organization and signaling (39). In present study, galectin-3 was upregulated in the upper villus of 21-day-old suckling piglets compared to the villus tip, while the expression of galectin-8 did not change. Loss of galectin-3 impairs membrane polarization of mouse enterocytes *in vivo* (40). This epitomizes the physiological importance of adequate provision of dietary amino acids for protein synthesis in the gut (41,42).

6. SUMMARY

We identified 194 BBM proteins during intestinal cell maturation along the jejunal crypt-villus axis in 21-day-old suckling piglets, and discovered 56 differentially expressed BBM proteins. Further characterization of these proteins in the BBM along the crypt-villus axis may help improve our understanding of the functions of enterocytes and provide targets for the regulation of intestinal cell proliferation and differentiation.

7. ACKNOWLEDGMENTS

Xia Xiong and Huansheng Yang contributed equally to this work. The research reported in the present study was supported by National Natural Science Foundation of China (31330075; 31301988; 31110103909; 31472106), State Key Laboratory of Animal Nutrition (2004DA125184F1304), Knowledge Innovation Program of Institute of Subtropical Agriculture, The Chinese Academy of Sciences (ISACX-LYQY-QN-1205), the Natural Science Foundation of Hubei Province (no. 2013CFA097 and 2013CFB325), the Hubei Hundred Talent program, and Texas A&M AgriLife Research (H-8200).

8. REFERENCES

1. Boudry G, Péron V, Le Huërou-Luron I, Lallès JP and Sève B: Weaning induces both

© 1996-2016

transient and long-lasting modifications of absorptive, secretory, and barrier properties of piglet intestine. *J Nutr* 134, 2256-62 (2004)
doi not found

2. Zabielski R, Godlewski MM and Guilloteau P: Control of development of gastrointestinal system in neonates. *J Physiol Pharmacol* 59, 35-54 (2008)
doi not found

3. Gerbe, F, Legraverend C and Jay P: The intestinal epithelium tuft cells: specification and function. *Cell Mol Life Sci* 69, 2907-17 (2012)
DOI: 10.1007/s00018-012-0984-7

4. Babyatsky M and Podolsky D: Growth and development of the gastrointestinal tract, in Textbook of gastroenterology; JB Lippincott Philadelphia. p. 547-584 (1999)
doi not found

5. Mariadason JM, Nicholas C, L'Italien KE, Zhuang M, Smartt HJ, Heerdt BG, Yang W, Corner GA, Wilson AJ, Klampfer L, Arango D and Augenlicht LH: Gene expression profiling of intestinal epithelial cell maturation along the crypt-villus axis. *Gastroenterology* 128, 1081-8 (2005)
DOI: 10.1053/j.gastro.2005.01.054

6. Fan MZ, Stoll B, Jiang R and Burrin DG: Enterocyte digestive enzyme activity along the crypt-villus and longitudinal axes in the neonatal pig small intestine. *J Anim Sci* 79, 371-81 (2001)
DOI: 2001/792371x

7. Gilbert ER, Williams PM, Ray WK, Li H, Emmerson DA, Wong EA and Webb KE Jr: Proteomic evaluation of chicken brush-border membrane during the early posthatch period. *J Proteome Res* 9, 4628-39 (2010)
DOI: 10.1021/pr1003533

8. Tan B, Yin YL, Liu ZQ, Li XG, Xu HJ, Kong XF, Huang RL, Tang WJ, Shinzato I, Smith SB, Wu GY: Dietary L-arginine supplementation increases muscle gain and reduces body fat mass in growing-finishing pigs. *Amino Acids* 37, 169-175 (2009)
DOI: 10.1007/s00726-008-0148-0

9. Kong XF, Tan BE, Yin YL, Li XL, Jaeger LA, Bazer FW, Wu GY: Arginine stimulates the mTOR signaling pathway and protein synthesis in porcine trophectoderm cells. J Nutr Biochem 23: 1178-1183 (2012)
DOI: 10.1016/j.jnutbio.2011.06.012

10. Yin YL, Yao K, Liu ZJ, Gong M, Ruan Z, Deng D, Tan BE, Liu ZQ and Wu GY: Supplementing L-leucine to a low-protein diet increases tissue protein synthesis in weanling pigs. *Amino Acids* 39, 1477-1486 (2010)
DOI: 10.1007/s00726-010-0612-5

11. Fan MZ, Matthews JC, Etienne NM, Stoll B, Lackeyram D and Burrin DG: Expression of apical membrane L-glutamate transporters in neonatal porcine epithelial cells along the small intestinal crypt-villus axis. *Am J Physiol Gastrointest Liver Physiol* 287, G385-G398 (2004)
DOI: 10.1152/ajpgi.00232

12. Zhou XH, Wu X, Yin YL, Zhang C and He LQ: Preventive oral supplementation with glutamine and arginine has beneficial effects on the intestinal mucosa and inflammatory cytokines in endotoxemic rats. *Amino Acids* 43, 813-821 (2012)
DOI: 10.1007/s00726-011-1137-2

13. Zeng GQ, Zhang PF, Deng X, Yu FL, Li C, Xu Y, Yi H, Li MY, Hu R, Zuo JH, Li XH, Wan XX, Qu JQ, He QY, Li JH, Ye X, Chen Y, Li JY and Xiao ZQ: Identification of candidate biomarkers for early detection of human lung squamous cell cancer by quantitative proteomics. *Mol Cell Proteomics* 11, M111. 013946 (2012)
DOI: 10.1074/mcp.M111.013946

14. Xiong X, Huang S, Zhang H, Li J, Shen J, Xiong J, Lin Y, Jiang L, Wang X and Liang S: Enrichment and proteomic analysis of plasma membrane from rat dorsal root ganglions. *Proteome Sci* 7, 41 (2009)
DOI: 10.1186/1477-5956-7-41

15. Tadjali M, Seidelin JB, Olsen J and Troelsen JT: Transcriptome changes during intestinal cell differentiation. *Biochim Biophys Acta* 1589, 160-7 (2002)
DOI: 10.1016/S0167-4889(02)00170-2

16. Suzuki T, Mochizuki K and Goda T: Localized expression of genes related to carbohydrate and lipid absorption along the crypt–villus axis of rat jejunum. *Biochim Biophys Acta* 1790, 1624-35 (2009)
DOI: 10.1016/j.bbagen.2009.08.004

17. Buhrke T, Lengler I and Lampen A: Analysis of proteomic changes induced upon cellular differentiation of the human intestinal cell line Caco□2. *Dev Growth Differ* 53, 411-26 (2011)
DOI: 10.1111/j.1440-169X.2011.01258.x

© 1996-2016

18. Hansson J, Panchaud A, Favre L, Bosco N, Mansourian R, Benyacoub J, Blum S, Jensen ON and Kussmann M: Time-resolved quantitative proteome analysis of in vivo intestinal development. *Mol Cell Proteomics* 10, M110. 005231 (2011) DOI: 10.1074/mcp.M110.005231

19. Dekaney CM, Wu GY, Yin YL and Jaeger LA: Regulation of ornithine aminotransferase gene expression and activity by all-transretinoic acid in Caco-2 intestinal epithelial cells. *J Nutr Biochem* 19, 674-681 (2008) DOI: 10.1016/j.jnutbio.2007.09.002

20. Hodin, RA, Chamberlain SM and Meng S: Pattern of rat intestinal brush-border enzyme gene expression changes with epithelial growth state. *Am J Physiol* 269, C385-C391 (1995) doi not found

21. Gabrilovac J, Cupić B, Zivković E, Horvat L and Majhen D: Expression, regulation and functional activities of aminopeptidase N (EC 3.4. 11.2; APN; CD13) on murine macrophage J774 cell line. *Immunobiology* 216, 132-44 (2011) DOI: 10.1016/j.imbio.2010.06.005

22. Ansorge S, Bank U, Heimburg A, Helmuth M, Koch G, Tadje J, Lendeckel U, Wolke C, Neubert K, Faust J, Fuchs P, Reinhold D, Thielitz A and Täger M: Recent insights into the role of dipeptidyl aminopeptidase IV (DPIV) and aminopeptidase N (APN) families in immune functions. *Clin Chem Lab Med* 47, 253-61 (2009) DOI: 10.1515/CCLM.2009.063

23. Goda T, Yasutake H, Tanaka T and Takase S: Lactase-phlorizin hydrolase and sucrase-isomaltase genes are expressed differently along the villus-crypt axis of rat jejunum. *J Nutr* 129, 1107-13 (1999) doi not found

24. Stahl A, Hirsch DJ, Gimeno RE, Punreddy S, Ge P, Watson N, Patel S, Kotler M, Raimondi A, Tartaglia LA and Lodish HF: Identification of the major intestinal fatty acid transport protein. *Mol Cell* 4, 299-308 (1999) DOI: 10.1016/S1097-2765(00)80332-9

25. Danielsen M, Hornshøj H, Siggers RH, Jensen BB, van Kessel AG and Bendixen E: Effects of bacterial colonization on the porcine intestinal proteome. *J Proteome Res* 6, 2596-04 (2007) DOI: 10.1021/pr070038b

26. Kent JC: How breastfeeding works. *J Midwifery Womens Health* 52, 564-70 (2007) DOI: 10.1016/j.jmwh.2007.04.007

27. Hwang ES, Hirayama BA and Wright EM: Distribution of the SGLT1 Na+ glucose cotransporter and mRNA along the crypt-villus axis of rabbit small intestine. *Biochem Biophys Res Commun* 181, 1208-17 (1991) DOI: 10.1016/0006-291X(91)92067-T

28. Iseki S, Kondo H, Hitomi M and Ono T: Localization of liver fatty acid-binding protein and its mRNA in the liver and jejunum of rats: an immunohistochemical and in situ hybridization study. *Mol Cell Biochem* 98, 27-33 (1990) DOI: 10.1007/BF00231364

29. Poirier H, Degrace P, Niot I, Bernard A and Besnard P: Localization and regulation of the putative membrane fatty acid transporter (FAT) in the small intestine. *Eur J Biochem* 238, 368-73 (1996) DOI: 10.1111/j.1432-1033.1996.0368z.x

30. Yang C, Albin DM, Wang Z, Stoll B, Lackeyram D, Swanson KC, Yin Y, Tappenden KA, Mine Y, Yada RY, Burrin DG and Fan MZ: Apical Na+-D-glucose cotransporter 1 (SGLT1) activity and protein abundance are expressed along the jejunal crypt-villus axis in the neonatal pig. *Am J Physiol Gastrointest Liver Physiol* 300, G60-G70 (2011) DOI: 10.1152/ajpgi.00208.2010

31. Levine DS and Woods JW: Immunolocalization of transferrin and transferrin receptor in mouse small intestinal absorptive cells. *J Histochem Cytochem* 38, 851-8 (1990) DOI: 10.1177/38.6.2186090

32. Rescher U, Ludwig C, Konietzko V, Kharitonenkov A and Gerke V: Tyrosine phosphorylation of annexin A2 regulates Rho-mediated actin rearrangement and cell adhesion. *J Cell Sci* 121, 2177-85 (2008) DOI: 10.1242/jcs.028415

33. Gerke V, Creutz CE and Moss SE: Annexins: linking Ca2+ signalling to membrane dynamics. Nat Rev Mol Cell Biol 6, 449-61 (2005) DOI: 10.1038/nrm1661

34. Friedrich T, Breiderhoff T and Jentsch TJ: Mutational analysis demonstrates that ClC-4 and ClC-5 directly mediate plasma membrane currents. *J Biol Chem* 274, 896-902 (1999) DOI: 10.1074/jbc.274.2.896

© 1996-2016

35. Clatworthy JP and Subramanian V: Stem cells and the regulation of proliferation, differentiation and patterning in the intestinal epithelium: emerging insights from gene expression patterns, transgenic and gene ablation studies. *Mech Dev* 101, 3-9 (2001) DOI: 10.1016/S0925-4773(00)00557-8

36. Beaulieu JF: Extracellular matrix components and integrins in relationship to human intestinal epithelial cell differentiation. *Prog Histochem Cytochem* 31, III-76 (1997) DOI: 10.1016/S0079-6336(97)80001-0

37. Schreider C, Peignon G, Thenet S, Chambaz J and Pinçon-Raymond M: Integrin-mediated functional polarization of Caco-2 cells through E-cadherin—actin complexes. *J Cell Sci* 115, 543-52 (2002) doi not found

38. Mandell KJ, Babbin BA, Nusrat A and Parkos CA: Junctional adhesion molecule 1 regulates epithelial cell morphology through effects on β1 integrins and Rap1 activity. *J Cell Biol* 280, 11665-74 (2005) DOI: 10.1074/jbc.M412650200

39. Garner OB and Baum LG: Galectin–glycan lattices regulate cell-surface glycoprotein organization and signalling. *Biochem Soc Trans* 36, 1472 (2008) DOI: 10.1042/BST0361472

40. Delacour D, Koch A, Ackermann W, Eude-Le Parco I, Elsässer HP, Poirier F and Jacob R: Loss of galectin-3 impairs membrane polarisation of mouse enterocytes in vivo. *J Cell Sci* 121, 458-465 (2008) DOI: 10.1242/jcs.020800

41. Wu G, Wu ZL, Dai ZL, Yang Y, Wang WW, Liu C, Wang B, Wang JJ and Yin YL: Dietary requirements of “nutritionally nonessential amino acids” by animals and humans. *Amino Acids* 44, 1107-1113 (2013) DOI: 10.1007/s00726-012-1444-2

42. Wu G: Dietary requirements of synthesizable amino acids by animals: A paradigm shift in protein nutrition. *J Anim Sci Biotechnol* 5, 34 (2014) DOI: 10.1186/2049-1891-5-34.

Abbreviations: APA: glutamyl aminopeptidase; APN: aminopeptidase N; BBM: brush-border membrane; BSA: bovine serum alumin; DPP IV: dipeptidyl peptidase 4; DTT: dithiothreitol; iTRAQ: isobaric tags for relative and absolute quantification; FABP 5: fatty acid binding protein 5; I-FABP: intestinal fatty acid binding protein; LC-MS/MS: liquid chromatography-tandem mass spectrometry; L-FABP: liver fatty acid binding protein; Na^+/K^+ ATPase: Na^+/K^+ -transporting ATPase; PMSF: phenylmethylsulfonyl fluoride

Key Words: Small Intestine; Proteomics; Villus-Crypt Axis; Suckling, Piglet

Send correspondence to: Yulong Yin, Research Center of Healthy Breeding of Livestock and Poultry and Key Laboratory for Agro-ecological Processes in Subtropical Region, Institute of Subtropical Agriculture, The Chinese Academy of Sciences, Hunan, China 410125, Tel: 86-731-84619703, Fax: 86-731-84612685, E-mail: yinyulong@isa.ac.cn

© 1996-2016